ERAU-PHY-0302

Oscillations and Cross Sections at the SNS with a Large Čerenkov Detector

Gordon J. VanDalen*

Department of Physics, Embry-Riddle Aeronautical University, Prescott, Arizona 86301

(Dated: February 3, 2008)

arXiv:nucl-ex/0309014v1 17 Sep 2003

Abstract

MiniBooNE at FermiLab should be able to confirm or refute the LSND Decay-in-Flight $\nu_\mu \to \nu_e$ oscillation signal within a few years. The primary evidence of neutrino oscillations from the LSND was in the anti-neutrino channel $\overline{\nu}_\mu \to \overline{\nu}_e$ channel, which may not be accessible at MiniBooNE for many years. The rates of signal and background are presented for a MiniBooNE style detector with a 250 ton mineral oil fiducial mass ($\sim$300m^3 fiducial volume) placed 60 meters from the Oak Ridge SNS beam stop. Several hundred $\overline{\nu}_\mu \to \overline{\nu}_e$ events could be measured in one beam year, even at the conservative end of the combined analysis of LSND and KARMEN. The same detector could easily measure neutrino-nucleus cross sections if filled with any interesting transparent fluid, several of which are suggested here. The rate and backgrounds for a methylene iodide filled detector are also presented as an example.

Talk at Neutrino Studies at the Spallation Neutron Source Workshop, August 28-29, 2003, Oak Ridge, TN.

*Electronic address: vanda029@erau.edu

I. INTRODUCTION

The LSND observation of anti-neutrino oscillations in the $\overline{\nu}_\mu \rightarrow \overline{\nu}_e$ channel [1] remains to be confirmed or refuted by an independent measurement. The LSND group also observed a statistically less robust signal for neutrino oscillations in a search for $\nu_\mu \rightarrow \nu_e$ candidates [2].

The MiniBooNE group at FermiLab is presently collecting data to test the LSND neutrino oscillation channel $\nu_\mu \rightarrow \nu_e$ using the ν_μ flux from the decay-in-flight (DIF) of a horn focused π^+ beam produced by 8 GeV protons [3]. Collection of the positive beam (neutrino) sample for their blind analysis will certainly take through 2004. The limited proton beam resources at FermiLab will be redirected in early 2005 [4] to other neutrino experiments [5]. This may not leave MiniBooNE enough beam to gather sufficient ν_μ data and still be able to switch horn polarity and collect data with the lower flux π^- DIF source of $\overline{\nu}_\mu$. MiniBooNE may end in the unsatisfactory condition of being unable to reach a strong conclusion about the primary LSND oscillation result in $\overline{\nu}_\mu \rightarrow \overline{\nu}_e$. Furthermore, the MiniBooNE signal to background ratio is expected to be less than one, even for for the higher flux π^+ DIF beam. The signal rate and quality are expected to be even less for the π^- DIF beam, should that configuration be run.

The Spallation Neutron Source (SNS) is presently under construction at Oak Ridge National Lab. [6] The SNS beam stop will provide a copious flux of decay-at-rest (DAR) neutrinos, primarily from π^+ and μ^+ decays. This neutrino source offers three major improvements over previous beam dump DAR neutrino sources. First, there will be a dedicated proton beam averaging 1.4 MW power operating throughout the year yielding a high total neutrino flux. Second, the beam spill comes within a 695ns interval corresponding to single turn extraction from the proton accumulator ring. This beam spill interval is less than the μ^+ life time of 2197 ns, but longer than the 26 ns π^+ life time, allowing good temporal separation of the ν_μ from π^+ decay and the $\nu_e + \overline{\nu}_\mu$ from μ^+ decay. Third, the recirculating liquid mercury beam stop quickly absorbs most π^- and μ^- before they decay at rest, greatly reduces DIF neutrino production, minimizing the associated backgrounds. The basic parameters of the initial SNS beam dump [7] neutrino source, and the higher energy source considered at the SNS^2 workshop [8] are given in Table I. The SNS began construction in 1999, and is scheduled for completion in 2006. Full operating intensity should be achieved by 2008, which is an appropriate time scale to build and commission the detector system

described here. An overview of the SNS site plan is shown in Fig. 1.

Perhaps more important than neutrino oscillation tests will be a wide range of neutrino-nucleus cross section measurements that can be made in the neutrino oscillation detector discussed here, and in a variety of dedicated single-purpose detectors placed closer to the SNS beam stop. The neutrino energies provided by the beam stop correspond well to the neutrino flux generated in Supernovæ, contributing to heavy element synthesis, the transfer of energy to outer layers of the star, and carrying away up to 99% of the energy released. This paper will also address how other transparent Čerenkov media might be used to measure neutrino-nucleus cross sections in a variety of elements using the SNS neutrino flux.

Previous studies of neutrino physics with the SNS [9] led to a white paper [10] and a proposal [11] for a large general facility known as ORLaND, the Oak Ridge Laboratory for Neutrino Detectors. A very large Čerenkov detector, ConDOR, of up to 2 kilotons mass was considered for precision standard model tests using neutrino-electron elastic scattering, and to study $\overline{\nu}_\mu \rightarrow \overline{\nu}_e$ oscillations to the 10^{-4} level. The detector presented here is much smaller than the CoNDOR/ORLaND design, and is focused on oscillation tests and neutrino-nucleus cross section measurements.

The Neutrino Studies at the Spallation Neutron Source (SNS^2) Workshop held August 28-29, 2003 at Oak Ridge [8], presents a new opportunity to bring neutrino physics to the great neutrino source that is being built at the SNS. The focus of the workshop was on physics with smaller detectors within the SNS Target building. Small scale segmented and homogenous detectors for neutrino-nucleus cross section measurements are being considered.

II. PROPOSED 250 TON DETECTOR

Why 60 meters?

Discussion has begun on neutrino detectors to be built within the SNS Target Hall itself, at about 22 meters from the beam stop [8]. Proposing a detector at 60 or more meters from the beam stop does make sense for several reasons. The SNS^2 site inside the Target Hall near the backward direction would offer about $4.5\times4.5\times6.5$ m^3 for all elements of two detectors, one homogenous and one fine grained. This volume needs to include passive shielding to filter the hadronic component of cosmic rays, active shielding to tag muons, and dead space

around the fiducial volume. Limitations on floor loading plus the passive and active shielding would limit the sensitive volume of a homogenous detector to at best 5 to 10 m^3 [12]. The tight confines would also limit access to detector elements, placing a premium on careful engineering.

A larger homogenous detector at about 60 meters from the beam stop would be outside the Target Hall and beyond the extended neutron beam lines in most directions (see Fig. 1). The loss in flux of a factor of about 7.5 would be easily compensated by the ability to make a much larger fiducial volume, at least 30 times greater in this proposal. Passive shielding, in the form of concrete blocks and earth, could be piled as high as needed to reduce cosmogenic backgrounds. 60 meters is, of course, a better distance to test and characterize the LSND anti-neutrino oscillation signal. The smaller SNS^2 homogenous detector within the Target Hall should also be built, as a near detector for the oscillation test, as a technology testbed for the larger detector, and as a less expensive platform for measuring larger neutrino-nucleus cross sections.

The proposed detector

This paper presents a medium scale detector which would be placed just below the ground surface at least 60 meters from the neutrino source. The detector would not impinge within 10 meters of the Target Hall foundations, and requires a final excavation only about 12% of the ORLaND scale. The Target Hall is shown in relation to the rest of the SNS site in Fig. 1. The Target Hall is 60 meters wide, with side walls 30 meters on either side of the beam dump. The detector presented here could definitively test the LSND $\overline{\nu}_\mu \rightarrow \overline{\nu}_e$ oscillation result, and also cover a range of interesting neutrino-nucleus scattering processes.

Both the original LSND experiment and MiniBooNE have shown that a large imaging Čerenkov detector can be operated under modest shielding near an accelerator. Other successful imaging Čerenkov detectors have operated deep underground primarily to reduce cosmic ray induced backgrounds to their non-accelerator physics processes.

A spherical 250 ton fiducial mass of mineral oil (density 860kg/m^3) would have a fiducial radius of 4.11m, occupying a volume of 291m^3. LSND and MiniBooNE restrict primary events to a fiducial volume 35cm inside the PMT faces. Allowing for an additional 35cm radius for the PMTs and their bases, another 25cm for an active a veto volume, and 5cm

for the combined thickness of the two tank walls, we get an outer detector radius of about 5.11 meters. The diameter would be about 33.5 feet, compared to the 40 foot diameter of MiniBooNE. A drawing of the proposed detector is presented in Fig. 2.

Two newer Hamamatsu photomultiplier tubes [13] offer better charge and time response than the original LSND PMT's (see Table II). Both LSND [14] and the Sudbury Neutrino Observatory [15] used R1408 eight-inch PMT's. The more efficient, better performing R5912 eight-inch PMT has replaced the R1408 in Hamamatsu's catalog. MiniBooNE uses several hundred R5912 8-inch PMTs among the older LSND tubes. The newer R8055 has a 13-inch photocathode. The number of tubes needed is calculated based on a 25% photocathode coverage as used by LSND to detect and resolve 2.2MeV gamma rays from neutron capture on free protons. MiniBooNE has about 10% photocathode coverage, allowing reconstruction of michel electrons from stopping muon decay, but cannot see the 2.2MeV neutron capture signal. Table II summarizes the properties of the R5912 and R8055 PMTs, and gives the number of each type required for 25% photocathode coverage in the proposed detector.

A 250 ton (fiducial) detector at the SNS filled with mineral oil, plus butyl-PBD to enhance scintillation light yield, would have 2.15×10^{31} free protons. (Which gives about half as many ^{12}C nuclei, 1.08×10^{31}. We also get 8.60×10^{31} atomic electrons.) We have used a 7% energy resolution for electrons at 50 MeV in the calculations below. The LSND detector with 1220 PMTs ultimately achieved an energy resolution of 7% at the michel endpoint of 52.8 MeV [16].

The original ORLaND facility proposal [11] for the SNS called for a hole in the ground 110 feet deep by 78 feet in diameter. This size was required to accomodate a 2kton detector plus several smaller detector for other neutrino-nucleus studies. The detector described here requires an excavation of at most 40 feet deep by 44 feet diameter, or about 12% of the volume of the whole ORLaND facility.

Shielding issues: passive and active

The detector could be built closer to ground level if sufficient earth for a passive hadron shield is piled overhead. LSND had a passive shield of 2000g/cm^2 [14], yielding a cosmic muon rate of 4kHz in the detector. MiniBooNE has 18 inches of concrete topped by at 3 meters of earth [3] for a total of at least 4000 g/cm^2 of passive shielding. MiniBooNE

experiences a cosmic muon rate of 9.2 kHz. The principle deadtime of both LSND and MiniBooNE, which use the same readout electronics, arises from a 15 μsec trigger hold-off after each muon. Greater passive shielding in the form of additional concrete and earth, plus newer readout and greater processing power, should allow a reduction in cosmic muon related deadtime.

LSND had a non-hermetic 15 cm thick liquid scintillator active veto inherited from the previous E-645 experiment [17], which has a veto inefficiency for charged particles of less than 10^{-5}. Gaps in this active veto led to problematic low energy neutron backgrounds from below which complicated initial oscillation analysis. MiniBooNE uses its working fluid of pure mineral oil without scintillation boosters to form an active veto volume 35 cm thick viewed by 240 PMTs. This hermetic system gives a veto efficiency of about 99.97%, at least an order of magnitude poorer than LSND's thinner liquid scintillator veto.

The proposed detector has double one-inch steel walls defining the outside of the detector, and the inner active volume. The veto and active volumes must be separated so that a highly responsive liquid scintillator can be used for an efficient veto for any liquid placed in the inner sensitive volume. This active veto would be 25 cm thick and hermetic, improving on both LSND and MiniBooNE experiences. The veto region can be viewed by several hundred 5-inch PMT's. Both the inner and outer wall of the veto region will be painted reflective white. The inner surface of the active volume will be painted a non-reflective black.

Detector efficiency $\varepsilon_{\rm rec}$

The LSND detector, operating with the same event energies expected here, had single electron reconstruction efficiencies which ranged from 40% to over 50% depending on the specific analysis. The poor duty factor of the LSND meant that stringent cuts needed to be applied to separate beam related electron events from non-beam backgrounds. The much lower duty factor of the SNS neutrino flux should allow a single electron efficiency well above 50%.

MiniBooNE faces a different set of problems while identifying electrons at about 500 MeV. Muons at this energy also produce Čerenkov cones, and the neutrinos are energetic enough to produce events with π^0s. A novel application of neural networks has allowed MiniBooNE to achieve an electron efficiency of at least 50% with good muon and π^0 rejection.

Neutron tagging, required for the anti-neutrino oscillation analysis, was complicated in the LSND by the backgrounds sneaking in through gaps in veto coverage. The proposed detector for the SNS must have an efficient hermetic veto system.

Although electron efficiencies well over 50% should be possible, we have chosen to parameterize our ignorance using a reconstruction efficiency $\varepsilon_{\rm rec}$ explicitly in all event rates given.

III. SNS NEUTRINO FLUXES, SHAPES AND RATIOS

At a nominal beam power of 1.4MW (1300 MeV kinetic energy protons) the SNS neutron source will also produce 2.92×10^{22} Decay-At-Rest (DAR) neutrinos (ν_μ, $\overline{\nu}_\mu$, and ν_e) per beam year. The search for $\overline{\nu}_\mu \to \overline{\nu}_e$ is based on the sequence shown here.

DAR in beam stop	oscillation in flight	in detector	
$\mu^+ \to {\rm e}^+\, \overline{\nu}_\mu\, \nu_e$	$\overline{\nu}_\mu \longrightarrow \overline{\nu}_e$	$\overline{\nu}_e\, {\rm p} \to {\rm n}\, {\rm e}^+$	${\rm n\ p} \to {\rm d}\ \gamma(2.2{\rm MeV})$
	$\longleftarrow$ 60 m $\longrightarrow$		detect e^+ followed by γ

The standard ORLaND neutrino flux plot is shown in Fig. 3. Similar plots have appeared in the ORLaND White Paper [10] and various proposal drafts. The White Paper [10] discusses a design using 1300 MeV protons on the SNS target, while a 1999 draft for a neutrino facility [11] shows this plot, but in the context of a 1000 MeV proton beam. The present SNS Parameters List (May 2003) [7] calls for a 1000 MeV beam. We use the SNS^2 Workshop [8] numbers for a 1300 MeV proton beam in what follows. However, a 1000 MeV proton beam would give a neutrino flux only about 5% lower. (See Table I.)

Each of the four flux components (ν_μ, $\overline{\nu}_\mu$, ν_e, $\overline{\nu}_e$) can be analyzed in terms of the parent processes to see what contribution comes from each decay source. The parent processes are sketched for SNS protons with a 1300 MeV kinetic energy in Fig. 4, adapted from Ref. [18].

The total event rate for one year then has essentially three time components.

- Beam unrelated (constant) background at a small rate measured in the 20μs before each beam spill
- A *prompt* component, in time with the beam spill, from $\pi^\pm$ DIF events, π^+ (ν_μ) DAR events, and the majority of the μ^- DAR (including about 70% of the intrinsic $\overline{\nu}_e$ background.

- A *decay* component, mostly following the muon DAR time scale, including ν_e ^{12}C events and the oscillation candidates.

The beam extraction from the storage ring will come in a single turn, roughly uniform in intensity over 695 ns [7]. The fraction of events within a prompt (0 to 695ns) and a muon decay (695ns to 5000ns) windows from the components above are given in Table III. The actual time distributions are illustrated in Fig. 5.

We can also estimate the timing of different event types since most of the π^+ decay at rest with life time of 26ns. About 98.5% of the π^- capture leaving only 1.5% to decay. The μ^+ decay at rest with life time 2197ns, while the μ^- capturing in the beam stop mercury have a life time of 76.2ns [19]. A fraction of the μ^- escape into lighter materials and decay/capture with the life time closer to the vacuum value.

The intrinsic oscillation background of $\overline{\nu}_e$ from μ^- DAR is suppressed by π^- and μ^- absorption in the mercury ($Z = 80$) beam stop. The total $\overline{\nu}_e$ fraction of 8.5×10^{-4} may be further reduced by requiring that events come after the 695ns beam spill.

The neutrino flux simulation shown in Fig. 3 was calculated with high-Z reflectors around the beam stop. The final design [7] uses beryllium reflectors, which will certainly raise the $\overline{\nu}_e$ backgrond, and diminish the potential gain from event time analysis. A new neutrino flux simulation with the final beam stop materials is needed to assess the final intrinsic $\overline{\nu}_e$ background, and what might be gained by using a time cut on the events to further suppress the $\overline{\nu}_e$ background.

The number of π^+ DAR and μ^+ DAR neutrinos produced is

$$N_\nu = (1.14 \times 10^{14}\text{p/pulse})(60\text{pulse/s})(3.16 \times 10^7\text{s/y})(0.135\ \nu\text{/p}) = 2.92 \times 10^{22}\nu\text{/beam year}$$

At 60m the neutrino flux per beam year would be $6.45 \times 10^{13}\nu/\text{cm}^2$.

IV. STANDARD EVENTS IN 250 TONS OF MINERAL OIL

We have used standard techniques to evaluate cross sections and event rates for neutrino-proton and neutrino-carbon interactions in a mineral oil filled detector. Both the $p(\overline{\nu}_e, e^+)n$ and $p(\overline{\nu}_\mu, \mu^+)n$ cross sections are calculated using the full expressions in Ref. [20], without low energy approximation. These calculations are equivalent to the program used by the

LSND Collaboration [21], but have been implemented in `Mathematica`, as have most of the calculations presented in this paper.

The standard electro-weak cross sections [22] have been used to evaluate rates for neutrino-electron elastic scattering.

The cross section for $^{12}\mathrm{C}(\nu_e, e^-)^{12}\mathrm{N}_{\mathrm{gs}}$ comes from Ref. [23], which has been cross checked with the LSND ν_e C results [24], and a table of equivalent cross sections in Ref. [25]. The cross section form for $^{12}\mathrm{C}(\nu_e, e^-)^{12}\mathrm{N}^*$ [25], has been cross checked with the LSND ν_e C results [24]. The cross sections for $^{12}\mathrm{C}(\nu, \nu')^{12}\mathrm{C}^*_{15.11}$ and $^{12}\mathrm{C}(\overline{\nu}, \overline{\nu}')^{12}\mathrm{C}^*_{15.11}$ are from Ref. [23], and have been compared to measurments by KARMEN [26]. The calculation [27] of $^{13}\mathrm{C}(\nu_e, e^-)X$ agrees well with both the KARMEN result [28] and the LSND final oscillation paper [16].

Finally, $^{12}\mathrm{C}(\nu_\mu, \mu^-)X$ and $^{12}\mathrm{C}(\overline{\nu}_\mu, \mu^+)X$ rates were scaled from the LSND results [29] correcting for the relative DIF fluxes and fiducial masses. Since the SNS DIF neutrino fluxes are also softer, due to the dense high-Z mercury target, these last calculations represent only upper limits. Event rates for fiducial mass of 250 tons of mineral oil, are summarized in Table IV.

V. THE $\overline{\nu}_\mu \to \overline{\nu}_e$ OSCILLATION SIGNATURE

The maximum mixing number of events for the LSND final event sample [16] was, for $T_e > 20$MeV, 33300 events. The maximum mixing events for a 250 ton (fiducial) detector at 60m from the SNS beam stop, using LSND reconstruction efficiency of 42%, would be 49500 events in one beam year. We have used the cross section for $p(\overline{\nu}_e, e^+)n$ from Refs. [20, 21]. Table V gives a comparison of the LSND parameters with the detector proposed here.

To calculate specific oscillation event rates, a set of *very conservative* oscillation parameters are taken from the combined analysis of both LSND and KARMEN by Church *et al.* [30]. The points in $\sin^2 2\theta$ and Δm^2 used in the calculations here are shown as crosses (+) in Figure 6. These points are, as can clearly be seen, conservative.

The three plots in Figure 7 show the smeared (7% at 50 MeV) energy distribution of events for each of the 3 cases considered. These are graphed directly in terms of events per MeV of energy per beam year.

VI. OSCILLATION BACKGROUNDS

The largest background comes from the residual $\overline{\nu}_e$ component of the beam. Fig. 8 shows the signal for the parameters of Fig. 7(b) with the intrinsic $\overline{\nu}_e$ background.

The other SNS beam related backgrounds come from misidentified DIF events, where the muon was missed. The energy distribution of these events comes simply from the michel electron spectrum. We can calculate the $p(\overline{\nu}_\mu, \mu^+)n$ background directly by requiring a muon kinetic energy below 3 MeV. The backgrounds from ν_μ ^{12}C and $\overline{\nu}_\mu$ ^{12}C are estimated from the scaled LSND backgrounds [29]. The total of these DIF backgrounds is less than 5 $\varepsilon_{\rm SNS}$ events per beam year.

The LSND experiment ran for approximately 15 months total over the years 1993-98, with a duty factor of about 0.06 imposed by the long beam pulse characteristic of LAMPF. The SNS beam duty factor is 4.2×10^{-5}, but the experiment must wait about 5 microseconds after each pulse starts to get most of the neutrino events from μ^+ DAR. This gives an *experimental* duty factor more like 3×10^{-4}. We can make a rough estimate the SNS beam-off background by scaling the LSND beam off background. The scaling factor is

$$\frac{[\text{duty factor(SNS)}]\ [\text{live time(SNS)}]\ M_{\rm SNS}\ \varepsilon_{\rm SNS}}{[\text{duty factor(LSND)}]\ [\text{live time(LSND)}]\ M_{\rm LSND}}\ \varepsilon_{\rm LSND} = \frac{(3\times10^{-4})(12\text{mo.})(250\text{tons})\ \varepsilon_{\rm SNS}}{(0.06)(15\text{mo.})(86.5\text{tons})(0.42)} = 0.0275\ \varepsilon_{\rm SNS}$$

The LSND experiment had 107 beam off events in the $R_\gamma > 1$ sample, which would give just 3 $\varepsilon_{\rm SNS}$ background beam off events in the SNS detector for one beam year.

The $\overline{\nu}_\mu \to \overline{\nu}_e$ oscillation backgrounds and signals are summarized in Table VI.

VII. $\nu_\mu \to \nu_e$ OSCILLATIONS

The LSND experiment was able to use the 3% π^+ DIF flux of ν_μ's to also search for $\nu_\mu \to \nu_e$ oscillations. The relatively high DIF flux was achieved by having a low-Z moderator (water) before a decay path and the final beam stop in 1993-95. The LSND *neutrino* oscillation paper [2] reported a result of modest statistical significance, oscillation probability of $(2.6 \pm 1.0 \pm 0.5) \times 10^{-3}$, even with their higher DIF ν_μ flux. With the lower DIF flux fractions at the SNS, the DIF oscillation rate is estimated at $6\varepsilon_{\rm rec}$ events with a negligible background.

It has been suggested [11] that DAR 29.8MeV ν_μ's from $\pi^+ \to \mu^+ \nu_\mu$ DAR could be detected after oscillation by the process

DAR in beam stop	oscillation in flight	in detector	
$\pi^+ \to \mu^+ \nu_\mu$	$\nu_\mu \longrightarrow \nu_e$	$\nu_e\ ^{12}\mathrm{C} \to e^-\ ^{12}\mathrm{N_{gs}}$	$^{12}\mathrm{N_{gs}} \to\ ^{12}\mathrm{C}\ e^+\ \nu_e$
	$\longleftarrow$ 60 m $\longrightarrow$		detect e^+ within 50ms

The oscillation event electrons come at about (29.8 - 16.8)MeV = 13MeV, spread by the energy resolution. So we are back in the traditional particle physics situation of looking for a "bump" on a known spectrum. Using the analytic cross section [23] for $^{12}\mathrm{C}(\nu_e, e^-)^{12}\mathrm{N_{gs}}$ we can calculate one of the backgrounds and the signal.

The largest beam related background is from DAR ν_e in the beam coming from $\mu^+ \to e^+\ \nu_e\ \overline{\nu}_\mu$ on a muon DAR time scale. Only about 14.3% of these events will come during the actual beam spill where we expect the signal from the oscillation of monochromatic 29.8MeV ν_μ from π^+ DAR.

We have plotted the signal and the $^{12}\mathrm{C}(\nu_e, e^-)^{12}\mathrm{N_{gs}}$ background in Fig. 9 for two different Δm^2 at $\sin^2 2\theta = 0.04$ which give a possible signal. Over the combined LSND/KARMEN allowed region [30] the size of the bump varies from a few up to $100\varepsilon_{\mathrm{rec}}$ events.

We have also calculated [23] the cross sections for $^{12}\mathrm{C}(\nu, \nu')^{12}\mathrm{C}^*_{15.11}$ where the 15 MeV gamma-ray could potentially present a large background to 13 MeV electron in this process. The KARMEN Collaboration measured [26, 28] the sum of the $\overline{\nu}_\mu$ and ν_e induced NC transitions to be $(10.9 \pm 0.7 \pm 0.8) \times 10^{-42}\mathrm{cm}^2$, consistent with our calculation which gives $9.86 \times 10^{-42}\mathrm{cm}^2$.

The total $^{12}\mathrm{C}(\nu, \nu')^{12}\mathrm{C}^*_{15.11}$ background in the beam window would be 14.3% of the μ^+ DAR events plus 96.3% of the π^+ DAR events, for a total of about 2760 $\varepsilon_{\mathrm{rec}}$ events. The LSND $^{12}\mathrm{C}(\nu_e, e^-)^{12}\mathrm{N_{gs}}$ analysis associated the $^{12}\mathrm{N_{gs}}$ decay betas with an efficiency of about 60% and an accidental background rate of about 0.5% of the remaining events. If we accept this accidental background rate, we would have about 15 $\varepsilon_{\mathrm{rec}}$ background events from accidentally associated $^{12}\mathrm{C}(\nu, \nu')^{12}\mathrm{C}^*_{15.11}$ background.

The DAR $\nu_\mu \to \nu_e$ process gives a signal bump of $(2 \to 100)$ $\varepsilon_{\mathrm{rec}}$ events with a beam related background bump of 15 $\varepsilon_{\mathrm{rec}}$ events from $^{12}\mathrm{C}(\nu, \nu')^{12}\mathrm{C}^*_{15.11}$ on top of a smooth background from $^{12}\mathrm{C}(\nu_e, e^-)^{12}\mathrm{N_{gs}}$ of about 15 $\varepsilon_{\mathrm{rec}}$ events per MeV. This DAR $\nu_\mu \to \nu_e$ measurement just might be possible if the mixing parameters are large enough.

VIII. OTHER LIQUIDS FOR THE DETECTOR

There are other amusing materials that one could use to fill all, or only a portion, of a large neutrino detector at the SNS. Then we could measure astrophysically interesting neutrino interactions with D, C, N, O, Cl, Br, I, etc. and others within the "imaging Čerenkov" detector technology.

With some imagination, and some materials testing, we could measure a variety of neutrino-nucleus cross sections with the SNS DAR neutrino fluxes. So long as the material is relatively inexpensive, respects the tank materials, and is not too hazardous, the concept of imaging Čerenkov can be taken well beyond the choice between water and oil. Table VII gives a short list of other potential liquids. Certainly there are many other liquids to consider as well.

Mineral oil (LSND and MiniBooNE) and water (SuperK, SNO, IMB) have relatively well known properties as a Čerenkov medium and for the liquid handling and purification requirements. SNO is also gaining experience with the use of dissolved salts (NaCl) to tag the presence of low energy neutrinos. Chlorine (^{35}Cl) has a high absorption cross-section for thermal neutrons, giving a gamma ray cascade peaked at around 8 MeV [15]. An SNS detector could use low concentrations of salts (as in SNO) to enhance neutron tagging in water, or could use higher concentrations of salt to provide other nuclear targets.

The simplest compound with nitrogen, ammonia (NH_3), has a boiling point of about -33°C. Mixtures of ammonia and water can give boiling points above 0°C. For example, a mixture of 90g NH_3 per 100g H_2O boils at 10°C. The DAR flux averaged cross section for $^{14}\mathrm{N}(\nu_e, e^-)^{14}\mathrm{O}$ is calculated at $29 \times 10^{-42}\mathrm{cm}^2$ [31], about twice the total ν_e ^{12}C cross section, and about three times the calculated total ν_e ^{16}O cross section [31]. Natural nitrogen is almost all ^{14}N with only 0.37% of ^{15}N.

Table VII gives other organic compounds containing at most one additional element. These liquids are transparent, have high index of refraction. Basic properties were gleaned from the CRC Handbook of Chemistry and Physics [32], the International Labor Organization International Safety Cards [33], the Atomic and Nuclear Properties of Matter from the PDG [34], and the NIST Stopping Power and Range Tables for Electrons [35]. Several of these materials are available in industrial amounts. Order by the "rail car" unit by checking the web for suppliers and quotes.

Tetrachlorethene (C_2Cl_4) was used in the Homestake solar neutrino detector by Ray Davis [36]. The common industrial use of tetrachlorethene was as a dry cleaning fluid, so it respects most artificial fibers used in clothing. The vapor of tetrachlorethene is heavier than air, and it suspected to be a carcinogen. There is no tolerance for any amount of spillage. Natural chlorine is roughly 3/4 ^{35}Cl and 1/4 ^{37}Cl. As noted above, ^{35}Cl has a high absorption cross-section for thermal neutrons, giving a gamma ray cascade peaked at around 8 MeV. The DAR flux averaged cross section for $^{37}\mathrm{Cl}(\nu_e, e^-)^{37}\mathrm{Ar}$ is calculated at $180 \times 10^{-42}\mathrm{cm}^2$ [37]. We would also need calculations of the ν_e ^{35}Cl cross section.

Methylene bromide (CH_2Br_2) is a commonly used industrial degreaser available in large amounts. Ethylene dibromide ($C_2H_4Br_2$, aka EDB) is used as an "octane" booster in aviation gas, and as a degreaser. Tribromoethene (C_2HBr_3) is rare and toxic. Bromine naturally occurs as about equal portions of ^{79}Br and ^{81}Br. Ref. [38] proposed using any of these same three liquids in the 380 m^3 tank of the Homestake Chlorine experiment [36] to also measure solar neutrinos. The ^{81}Kr would have been detected by resonance ionization spectrometry rather than by radiochemical means. The DAR flux averaged cross section for $^{81}\mathrm{Br}(\nu_e, e^-)^{81}\mathrm{Kr}$ is calculated at $450 \times 10^{-42}\mathrm{cm}^2$ [37]. Cross section estimates are also needed for ν_e ^{79}Br.

Ethyl iodide (C_2H_5I) is used in small amounts with ^{14}C as a radiochemical tag in metabolism studies. Methylene iodide (CH_2I_2) is prized for its high index of refraction, used in the gemstone industry for immersion tests to quickly sort materials. Both materials will darken (iodine liberated) upon exposure to light. Natural iodine is 100% ^{127}I. Cross sections for ν_e ^{127}I will be discussed in the next section where event rates in a methylene iodide detector are presented.

All organic compounds listed are solvents which could easily be doped with butyl-PBD to enhance scintillation light yield. C_2Cl_4 could be added to provide ^{35}Cl to tag neutrons associated with primary neutrino interactions.

Finally, heavy water D_2O could be placed in a transparent subvolume within a water filled detector. D_2O does have a specific gravity 10.5% greater than water, so this would need to be a substantial transparent containment vessel. This same system, if strong enough could also hold subvolumes of other expensive liquids where the cross sections are expected to be high enough to eliminate the need for filling the full fiducial volume.

How would Hamamatsu feel about having their PMT's in ammonia at -40°C? Have people

tested tubes in any other materials like these? Cables? Paints? Other tank materials? A good summer student project would be to measure optical properties and PMT responses for these and other organic solvents.

IX. RATES FOR METHYLENE IODIDE CH_2I_2

The charged current cross section for ν_e ^{127}I could be measured quickly by filling the inner volume of the detector with methylene iodide. Within the fiducial volume there would be 967,000 kg or 967 tons of material. (Our "250 ton" size only applies to mineral oil.) The fiducial volume then contains 2.17×10^{30} CH_2I_2 molecules. With 2 iodine atoms per molecule, there are 4.35×10^{30} iodine atoms in the fiducial volume.

Iodine has just one stable isotope, namely ^{127}I. The threshold neutrino energy for $^{127}\mathrm{I}(\nu_e, e^-)^{127}\mathrm{Xe}$ is 0.789MeV. For excitation energies above about 8 MeV the ^{127}Xe nucleus is unstable to neutron emission. An experiment run at LANL [39] measured the rate for

$$\nu_e\ ^{127}\mathrm{I} \rightarrow\ ^{127}\mathrm{Xe}_{\text{bound states}} e^- \qquad \Longrightarrow \qquad ^{127}\mathrm{Xe}_{\text{gs}}$$

where the $^{127}\mathrm{Xe}_{\text{gs}}$ was detected radio-chemically by its 36.4 day half-life electron capture decay back to ^{127}I. The measured cross section is $(2.75 \pm 0.84 \pm 0.24) \times 10^{-40}\mathrm{cm}^2$. A theoretical calculation [40] for the same exclusive process gave $(2.1 \rightarrow 3.1) \times 10^{-40}\mathrm{cm}^2$. Ref. [37] calculates that the *total* ν_e ^{127}I cross section is about 70% higher than that for the bound states. The proposed SNS detector discussed here could get 131,000 ε_{rec} $^{127}\mathrm{I}(\nu_e, e^-)X$ events per beam year.

The event rate for ν_e C charged currents can be calculated, being careful that there is but one carbon atom for every two iodine atoms in methylene iodide. The event rates for the methylene iodide filled detector are summarized in Table VIII. The 131,000 ν_e ^{127}I events should stand out clearly.

There do not appear to be any short lived betas in the $A = 127$ system (half-life less than 100 milliseconds), but the detector could tag additional excited states through prompt neutron emission or gammas. Radiochemical experiments can measure the cross section which leads to the ^{127}Xe bound states, but an imaging Čerenkov detector can measure differential cross sections in electron energy and angle, as well as tag excited states with emitted neutrons and/or gammas. The SNS neutrino physicists need guidance on both

semi-inclusive and total cross sections for ν ^{127}I charged and neutral currents. The detector could be sensitive to prompt neutrons and gammas, as well as delayed gammas and betas on the time scales from 10 microseconds to 100 milliseconds.

Although the event rate for methylene iodide is quite large, other materials suggested in the previous section would give between a few thousand and tens of thousands of events per beam year.

X. CONCLUSION

$\overline{\nu}_\mu \rightarrow \overline{\nu}_e$ oscillation event rate for $\Delta m^2 < 0.5\text{eV}^2$ will be a factor of about **four** enhanced relative to conventional processes due to the doubling of L from 30 meters used by LSND to 60 meters as proposed here.

A 250 ton detector placed 60 meters from the SNS mercury beam stop can easily confirm or refute the LSND $\overline{\nu}_\mu \rightarrow \overline{\nu}_e$ oscillation signal within one nominal beam year of data taking. The backgrounds are much less than at the LSND experiment, and signals over the LSND/KARMEN low Δm^2 allowed region will be several hundred events. The same experiment can improve previous measurements of ν_e ^{12}C charged current, ν ^{12}C neutral current, and ν e elastic cross sections with DAR neutrinos. Moving the detector futher away from the beam stop, out to 100 meters, decreases the rate from conventional processes as $1/r^2$, while oscillation signal rates remain roughly constant for $\Delta m^2 \leq 0.3\text{eV}^2$.

The detector can also study other neutrino-nucleus cross sections with high statistics using other liquids. This can be a long lived experiment as different liquids are studied in turn.

Acknowledgements

First, I would like to thank Prof. Darrel Smith and my colleagues at Embry-Riddle Aeronautical University for providing me a new home in retirement. Thanks also to the organizers of the Neutrino Studies at the Spallation Neutron Source Workshop held August 28-29, 2003 at Oak Ridge National Lab for giving me a chance to present these ideas. Their work to prepare an SNS[2] proposal will bring neutrino physics to what soon will be our best neutrino source. Also, my thanks to Yuri Efremenko, Bill Louis, and Ion Stancu for their

comments and encouragement. Finally I acknowledge all the work which has gone before on neutrino physics at the SNS, particularly for the persistence and leadership of Frank Avignone.

---

[1] C. Athanassopoulos *et al.* (LSND Collaboration), *"Evidence for $\overline{\nu}_\mu \to \overline{\mu}_e$ oscillation from the LSND experiment at the Los Alamos Meson Physics Facility,"* Phys. Rev. Lett. **77**, 3082-3085 (1996) nucl-ex/9605003.

C. Athanassopoulos *et al.* (LSND Collaboration), *"Evidence for neutrino oscillations from muon decay at rest,"* Phys. Rev. **C54** 2685-2708 (1996)nucl-ex/9605001.

[2] C. Athanassopoulos *et al.* (LSND Collaboration), *"Results on $\nu_\mu \to \nu_e$ Neutrino Oscillations from the LSND Experiment",* Phys. Rev. Lett. **81**, 1774-1777 (1998) nucl-ex/9709006.

C. Athanassopoulos *et al.* (LSND Collaboration), *"Evidence for $\nu_\mu \to \nu_e$ oscillations from pion decay in flight neutrinos,"* Phys. Rev. C **58**, 2489 (1998) nucl-ex/9706006.

[3] E. Church *et al.* BooNe Collaboration, *"A proposal for an experiment to measure $\nu_\mu \to \nu_e$ oscillations and muon-neutrino disappearance at the Fermilab Booster: BooNE,"* FERMILAB-PROPOSAL-0898.

See also the web site `http://www-boone.fnal.gov/`

[4] The June 2003 Fermilab PAC meeting notes discuss "Proton Economics" on page 14. The full report is available at `http://www.fnal.gov/directorate/program_planning/phys_adv_com/PACJune03PUBLIC.pdf`

The long range Fermilab beams schedule at this writing has the MiniBooNE beam shut off at the end of 2004. MINOS then comes online for commissioning at the start of 2005.

This would at best bring MiniBooNE close to the 1×10^{21} protons on target for their initial neutrino (ν_μ) data sample. MiniBooNE can also double its decay path, and would need many more protons on target to complete an anti-neutrino ($\overline{\nu}_\mu$) sample.

[5] E. Ables *et al.* [MINOS Collaboration], *"P-875: A Long baseline neutrino oscillation experiment at Fermilab,"* FERMILAB-PROPOSAL-0875

MINOS is presently taking cosmic data, and is ready for beam. See Kurt Riesselmann, *"Startup of MINOS Half a Mile Underground",* FermiNews, Vol. 26, No. 13, September 2003.

See also the NuMI/MINOS web site ar `http://www-numi.fnal.gov`

[6] The Spallation Neutron Source (SNS) is an accelerator-based neutron source being built in Oak Ridge, Tennessee, by the U.S. Department of Energy. `http://www.sns.gov/`

[7] *"SNS Parameters List"*, SNS 100000000-PL0001-R09, May 2003 (available on the web as `http://www.sns.gov/documentation/100000000-PL0001-R09.pdf`)

[8] Neutrino Studies at the Spallation Neutron Source Workshop: August 28-29, 2003, Oak Ridge, Tennessee, `http://www.phy.ornl.gov/workshops/sns2/`

[9] W. Bugg *et al.*, *"Orlando: Oak Ridge Large Neutrino Detector,"* Nucl. Phys. Proc. Suppl. **70** (1999) 472.

[10] *"Scientific Opportunities at the Oak Ridge Laboratory for Neutrino Detectors (ORLaND)",* May 2000.

[11] *"A Large Neutrino Detector Facility at the Spallation Neutron Source at Oak Ridge National Laboratory",* Draft 3.1, Feb. 12, 1999.

See also F. T. Avignone *et al.*, *"Orland: A Proposed Neutrino Facility At The Oak Ridge National Laboratory,"* Phys. Atom. Nucl. **63** (2000) 1007 [Yad. Fiz. **63** (2000) 1082].

[12] I. Stancu, *"Homogenous Detectors: Technology and Performance",* talk given at the SNS^2 workshop. See `http://www.phy.ornl.gov/workshops/sns2/Stancu.pdf`

[13] See the Hamamatsu web site at `http://usa.hamamatsu.com/` Data sheets for the two PMTs are at `http://usa.hamamatsu.com/hcpdf/parts_R/R5912.pdf` and `R8055.pdf`

[14] C. Athanassopoulos *et al.* (LSND Collaboration), *"The Liquid Scintillator Neutrino Detector and LAMPF Neutrino Source,"* Nucl. Instrum. Meth. A **388**, 149 (1997) nucl-ex/9605002.

[15] J. Boger *et al.* (SNO Collaboration), *"The Sudbury Neutrino Observatory",* Nucl. Instrum. Meth. A **449**, 172 (2000) nucl-ex/9910016.

[16] A. Aguilar, *et al.* (LSND Collaboration) *"Evidence for Neutrino Oscillations from the Observation of $\overline{\nu}_e$ in a $\overline{\nu}_\mu$ Beam",* Phys.Rev. **D64**, 112007 (2001) hep-ex/0104049.

[17] J. J. Napolitano *et al.*, *"Construction And Performance Of A Large Area Liquid Scintillator Cosmic Ray Anticoincidence Detector,"* Nucl. Instrum. Meth. A **274**, 152 (1989).

[18] Yuri Efremenko, *"Stellar Neutrino Studies at the Spallation Neutron Source (Oak Ridge)",* Talk presented at the 5$^{\text{th}}$ International Conference of Neutrino Factories and Superbeams, Columbia University, 5-11, June 2003.

`https://www2.bnl.gov/cap/nufact03/WG2/10june/efremenko.ppt`

[19] T. Suzuki, D.F. Measday and J.P. Roalsvig, *"Total nuclear capture rates for negative muons",*

Phys. Rev. **C35**, 2212 (1987)

[20] P. Vogel, *"Analysis of the antineutrino capture on protons",* Phys. Rev. **D29**, 1918 (1984)

[21] William C. Louis, private communication

[22] D.E. Groom *et al.*, The European Physical Journal **C15**, 1 (2000), and 2001 off-year partial update for the 2002 edition available on the PDG WWW pages (URL: `http://pdg.lbl.gov/`)

[23] M. Fukugita, Y. Kohyama, K. Kubodera, *"Neutrino Reaction Cross-Sections On ^{12}C Target"*, Phys. Lett. **B212**, 139 (1988)

[24] L. Auerbach *et al.* (LSND Collaboration), *"Measurements of Charged Current Reactions of ν_e on ^{12}C",* Phys. Rev. **C64**, 065501 (2001) hep-ex/0105068.

[25] E. Kolbe, K. Langanke, F.-K. Theilmann, and P. Vogel, *Inclusive* $^{12}\mathrm{C}(\nu_\mu,\mu)^{12}\mathrm{N}$ *reaction in the continuum random phase approximation",* Phys. Rev. **C52**, 3437 (1995)

[26] B. Armbruster *et al.* (KARMEN Collaboration), *"Measurement of the weak neutral current excitation* $^{12}\mathrm{C}(\nu_\mu,\nu'_\mu)^{12}\mathrm{C}^*(1^+,1;15.1MeV)$ *at* $E(\nu_\mu) = 29.8MeV$*",* Phys. Lett. **B423**, 15-20 (1998)

[27] M. Fukugita, Y. Kohyama, K. Kubodera, and T. Kuramoto, *"Reaction cross sections for* $\nu\ ^{13}\mathrm{C} \to e^-\ ^{13}\mathrm{N}$ *and* $\nu\ ^{13}\mathrm{C} \to \nu'\ ^{13}\mathrm{C}^*$ *for low energy neutrinos"*, Phys. Rev. **C13**, 1359 (1990)

[28] Reinhard Maschuw *et al.* (KARMEN Collaboration), *"Neutrino Spectroscopy with KARMEN"*, Prog. Part. Nucl. Phys. **40**, 183 (1998)

[29] L. Auerbach *et al.* (LSND Collaboration), *"Measurements of Charged Current Reactions of ν_μ on ^{12}C",* Phys. Rev. **C66**, 015501 (2002) nucl-ex/0203011.

[30] E. D. Church, K. Eitel, G. B. Mills, and M. Steidl, *"Statistical analysis of different* $\overline{\nu}_\mu \to \overline{\nu}_e$ *searches",* Phys. Rev. **D 66**, 013001 (2002) hep-ex/0203023.

[31] N. Auerbach and B. A. Brown, *"Weak interaction rates involving ^{12}C, ^{14}N, and ^{16}O,"* Phys. Rev. C **65**, 024322 (2002).

[32] *"The CRC Handbook of Chemistry and Physics",* 50th Edition, Robert C. Weast, editor, The Chemical Rubber Co., Cleveland, Ohio, 1969.

[33] *"International Labor Organization International Chemical Safety Cards (ICSC)",* web site at `http://www.ilo.org/public/english/protection/safework/cis/products/icsc`

[34] *"Atomic and Nuclear Properties of Matter from the Particle Data Group",* web site at `http://pdg.lbl.gov/AtomicNuclearProperties/`

[35] *"The NIST Stopping Power and Range Tables for Electrons - ESTAR",* web site at

http://physics.nist.gov/PhysRefData/Star/Text/ESTAR.html

[36] R. J. Davis, D. S. Harmer and K. C. Hoffman, *"Search For Neutrinos From The Sun,"* Phys. Rev. Lett. **20**, 1205 (1968).

[37] T. S. Kosmas and E. Oset, *"Charged Current Neutrino Nucleus Reaction Cross-Sections At Intermediate-Energies,"* Phys. Rev. C **53** (1996) 1409.

[38] G. S. Hurst, C. H. Chen, S. D. Kramer, B. T. Cleveland, R. Davis, J. K. Rowley and F. J. Schima, *"Feasibility Of A* $^{81}\mathrm{Br}(\nu, e^-)^{81}\mathrm{Kr}$ *Solar Neutrino Experiment,"* Phys. Rev. Lett. **53** (1984) 1116.

[39] J.R. Distel *et al.*, *"Measurement of the cross section for the reaction* $^{127}\mathrm{I}(\nu_e, e)^{127}\mathrm{Xe}_{\text{bound states}}$ *with neutrinos from the decay of stopped neutrinos",* nucl-ex/0208012.

[40] J. Engel, S. Pittel, P. Vogel, *"Capture of Solar and Higher Energy Neutrinos by Iodine 127",* Phys. Rev. **C50**, 1702-1708 (1994) nucl-th/9402022.

TABLE I: Key SNS Parameters.

SNS Parameter	**SNS Parameters List [7]**	**SNS^2 Workshop [8]**
beam power on target	1.4 MW	1.4 MW
beam energy on target	1 GeV	1.3 GeV
repetition rate	60 Hz	60 Hz
protons per pulse	1.6×10^{14}	1.14×10^{14}
extracted pulse length	695 nsec	695 nsec
target	mercury	mercury
beam spot on target	7cm × 20cm (V×H)	7cm × 20cm (V×H)
DAR neutrinos per proton	0.098ν/p	0.135ν/p
DAR neutrinos per beam year	2.78×10^{22} ν	2.92×10^{22} ν

TABLE II: Two Hamamatsu Phototubes for the SNS Čerenkov Detector

	R5912	**R8055**
height	290 mm	332 mm
diameter	202 mm	332 mm
effective diameter	190 mm	325 mm
quantum efficiency at 390nm	22%	20%
spectral response	300 to 650 nm	
peak sensitivity	420 nm	
typical HV for 10^7 gain	1500 volts	
transit time spread (FWHM)	2.4 ns	2.8 ns
number for 25% photocathode coverage	2106	720

TABLE III: Event fractions in time windows

event types	$0 \rightarrow 0.695\mu$sec	$0.695 \rightarrow 5\mu$sec	$> 5\mu$sec
π^+ DAR and $\pi^\pm$ DIF events	96.3%	3.7%	0
μ^+ DAR and oscillation candidates	14.3%	73.6%	12.1%

TABLE IV: Event Rates in 250tons of Mineral Oil

Process	Neutrino Source	ν Source Life Time	Total Events per Beam Year
$\nu_\mu\ e$	π^+ DAR	26ns	69 $\varepsilon_{\rm rec}$
$\overline{\nu}_\mu\ e$	μ^+ DAR	2197ns	99 $\varepsilon_{\rm rec}$
$\nu_e\ e$	μ^+ DAR	2197ns	630 $\varepsilon_{\rm rec}$
Total $\nu\ e$ events $T_e > 20$MeV			**798** $\varepsilon_{\rm rec}$
$^{12}{\rm C}(\nu_e, e^-)^{12}{\rm N}_{\rm gs}$	μ^+ DAR	2197ns	4689 $\varepsilon_{\rm rec}$
$^{12}{\rm C}(\nu_e, e^-)^{12}{\rm N}^*$	μ^+ DAR	2197ns	2147 $\varepsilon_{\rm rec}$
$^{13}{\rm C}(\nu_e, e^-)X$	μ^+ DAR	2197ns	308 $\varepsilon_{\rm rec}$
Total ν_e C events $T_e > 20$MeV			**7144** $\varepsilon_{\rm rec}$
$^{12}{\rm C}(\nu_\mu, \nu_\mu)^{12}{\rm C}^*_{15.11}$	π^+ DAR	26ns	1851 $\varepsilon_{\rm rec}$
$^{12}{\rm C}(\overline{\nu}_\mu, \overline{\nu}_\mu)^{12}{\rm C}^*_{15.11}$	μ^+ DAR	2197ns	3752 $\varepsilon_{\rm rec}$
$^{12}{\rm C}(\nu_e, \nu_e)^{12}{\rm C}^*_{15.11}$	μ^+ DAR	2197ns	3093 $\varepsilon_{\rm rec}$
Total ν_e C NC events			**8696** $\varepsilon_{\rm rec}$
$^{12}{\rm C}(\nu_\mu, \mu^-)X$	π^+ DIF	26ns	≤ 278 $\varepsilon_{\rm rec}$
$^{12}{\rm C}(\overline{\nu}_\mu, \mu^+)X$	π^- DIF	26ns	≤ 82 $\varepsilon_{\rm rec}$
$p(\overline{\nu}_\mu, \mu^+)n$	π^- DIF	26ns	272 $\varepsilon_{\rm rec}$

TABLE V: Comparison of LSND and 250 ton SNS Detector Both with Efficiency $\varepsilon = 0.42$

parameter	LSND (1993-98)	SNS 250 ton detector
beam kinetic energy	798 MeV	1300 MeV
ν/p	0.079	0.135
fiducial mass	86.5 tons	250 tons
free protons N_t	7.4×10^{30}	4.3×10^{31}
ν flux	$1.26 \times 10^{14} \nu/\mathrm{cm}^2$	$6.45 \times 10^{13} \nu/\mathrm{cm}^2$/year
ν flight path L	30m	60m
Maximum mixing events ($\varepsilon = 42\%$)	33,300	49,500 / beam year
beam duty factor	6×10^{-2}	4.2×10^{-5}

TABLE VI: Oscillation Event Rates and Backgrounds in 250tons of Mineral Oil

DAR $\overline{\nu}_\mu \to \overline{\nu}_e$ Oscillation Signal Event Rates		
($\sin^2 2\theta$,Δm^2)		Events
(0.0025,1 eV^2)		266 $\varepsilon_{\mathrm{rec}}$
(0.0075,0.5 eV^2)		592 $\varepsilon_{\mathrm{rec}}$
(0.040,0.2eV^2)		693 $\varepsilon_{\mathrm{rec}}$
DAR $\overline{\nu}_\mu \to \overline{\nu}_e$ Oscillation Background Event Rates		
Intrinsic $\overline{\nu}_e$	8.5×10^{-4} per DAR ν	81 $\varepsilon_{\mathrm{rec}}$
ν_μ ^{12}C	π^+ DIF	< 0.15 $\varepsilon_{\mathrm{rec}}$
$\overline{\nu}_\mu$ ^{12}C	π^- DIF	≤ 0.3 $\varepsilon_{\mathrm{rec}}$
$\overline{\nu}_\mu$ p	π^- DIF	4.4 $\varepsilon_{\mathrm{rec}}$
mis-ID μ, μ behind PMT		< 0.5 $\varepsilon_{\mathrm{rec}}$
Beam Off ($R_\gamma > 1$)		3 $\varepsilon_{\mathrm{rec}}$

TABLE VII: Possible Čerenkov Liquids. Information from Refs. [32, 33, 34, 35]

					Radiation 50MeV e^-			
Physics	Stuff	Chemical	Density	n_D	Length	Range	M.P.	B.P.
ν_e C CC	mineral oil	C_nH_{2n+2}	860kg/m^3	1.47	44.8g/cm^2	14.8g/cm^2		>150°C
ν C NC		$n \simeq 20$				add butyl-PBD for n's		
ν_e O CC	water	H_2O	1000kg/m^3	1.33	36.1g/cm^2	19.8g/cm^2	0°C	100°C
ν O NC						add Gd or NaCl to see n's?		
ν N	ammonia	NH_3	771kg/m^3	1.33	41g/cm^2	16.8g/cm^2		−33°C
	ammonia+water	(90g NH_3 per 100g H_2O at 10°C)				add H_2O for room temp liquid		
ν Cl	tetrachloroethene	C_2Cl_4	1625kg/m^3	1.51	21g/cm^2	19.8g/cm^2	−19°C	121°C
ν Br	tribromoethene	C_2HBr_3	2708kg/m^3	1.604	12.3g/cm^2	17.3g/cm^2		163°C
ν Br	methylene bromide	CH_2Br_2	2497kg/m^3	1.542	12.2g/cm^2	15.7g/cm^2	−53°C	97°C
ν Br	ethylene dibromide	$C_2H_4Br_2$	2179kg/m^3	1.534	12.9g/cm^2	15.5g/cm^2	10°C	131°C
ν I	ethylene iodide	$C_2H_5I_1$	1936kg/m^3	1.742	10.0g/cm^2	15.0g/cm^2	−108°C	73°C
ν I	methylene iodide	CH_2I_2	3325kg/m^3	1.742	8.9g/cm^2	15.1g/cm^2	6.1°C	182°C
ν D	deuterated water	D_2O	1105kg/m^3	1.34		transparent sub-volume		

TABLE VIII: Event rates in a methylene iodide filled detector

Process	σ	Events per beam year
$^{127}\mathrm{I}(\nu_e, e^-)^{127}\mathrm{Xe}_{\text{bound states}}$	$2.75 \times 10^{-40}\mathrm{cm}^2$	**77,000** ε_{rec}
$^{127}\mathrm{I}(\nu_e, e^-)^{127}\mathrm{Xe}^*_{\text{total}}$		**131,000** ε_{rec}
$^{127}\mathrm{I}(\nu_e, e^-)X\ n$	?	?
$^{127}\mathrm{I}(\nu, \nu')^{127}\mathrm{I}^*$	?	?
$^{12}\mathrm{C}(\nu_e, e^-)^{12}\mathrm{N}_{\text{gs}}$	$6.76 \times 10^{-42}\mathrm{cm}^2$	946 ε_{rec}
$^{12}\mathrm{C}(\nu_e, e^-)^{12}\mathrm{N}^*$	$5.41 \times 10^{-42}\mathrm{cm}^2$	602 ε_{rec}
$^{13}\mathrm{C}(\nu_e, e^-)X$	$50 \times 10^{-42}\mathrm{cm}^2$	78 ε_{rec}
$\mathrm{C}(\nu_e, e^-)X$ total		**1626** ε_{rec}

FIG. 1: The SNS Site.

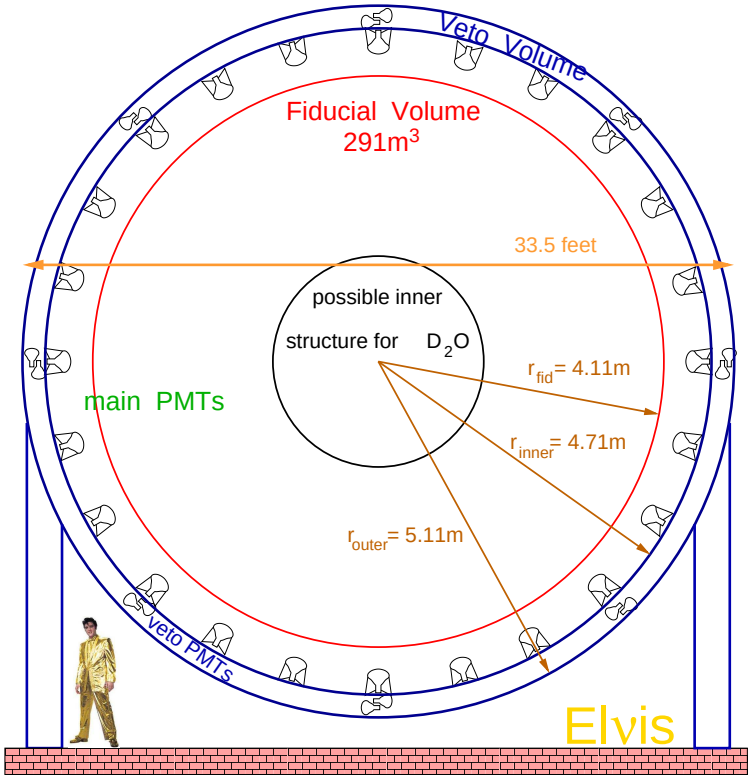

FIG. 2: Proposed SNS Detector. El$\nu$is: (Exchangeable Liquid Neutrino Imaging System)

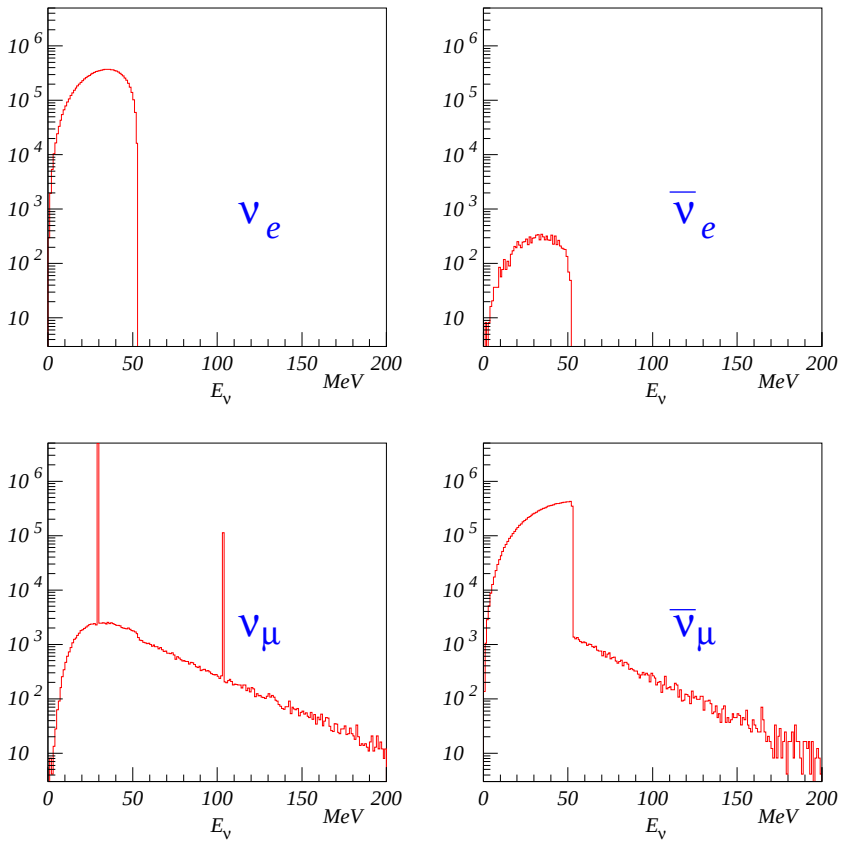

FIG. 3: Neutrino energy distributions from the SNS mercury beam stop. Adapted from Ref. [18].

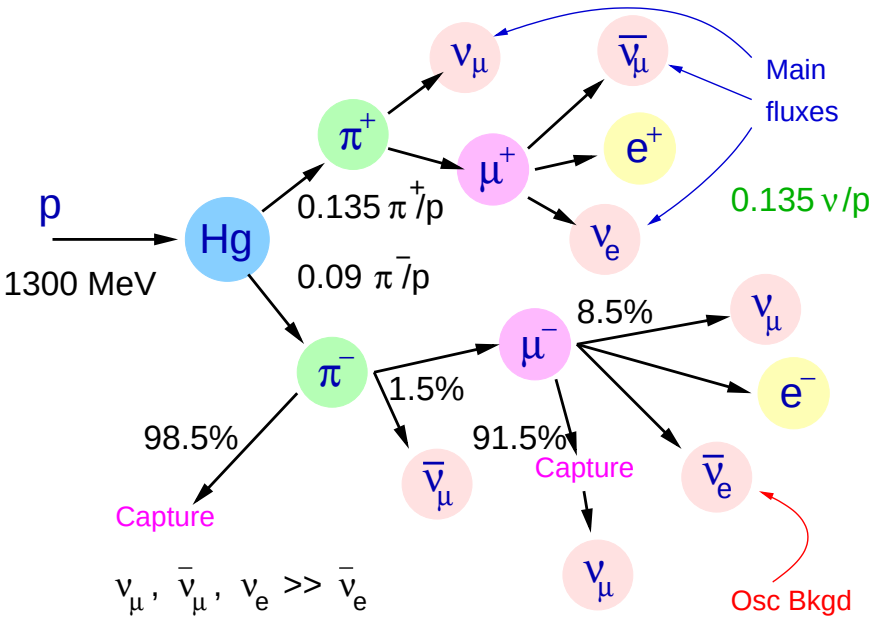

FIG. 4: Neutrino production in the SNS mercury beam stop. Adapted from Ref. [18].

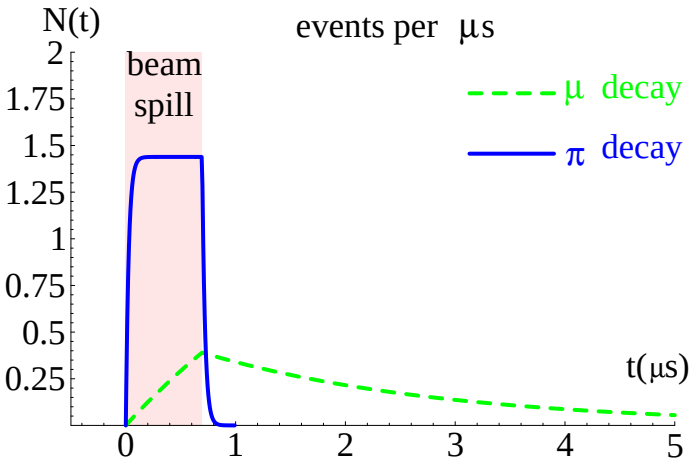

FIG. 5: Neutrino production time distribution.

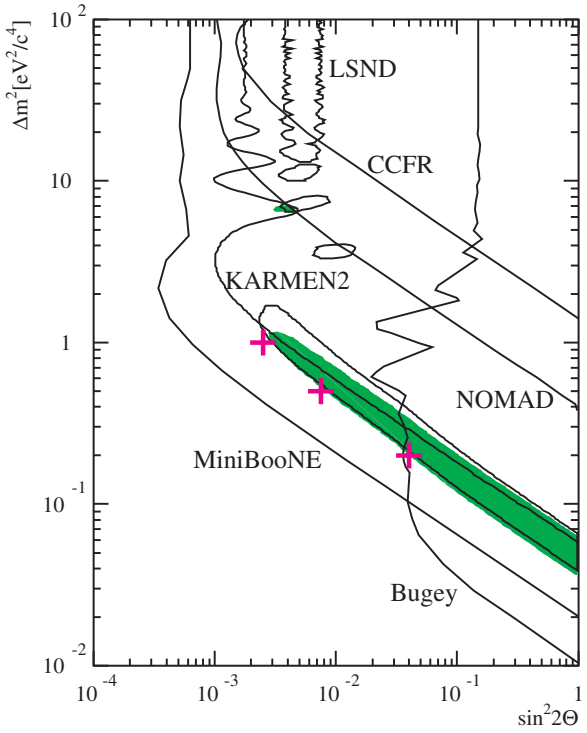

FIG. 6: Region in Δm^2 vs. $sin^2 2\theta$ from a combined analysis of LSND and KARMEN [30]. The crosses show three conservative oscillation parameter sets considered in this paper.

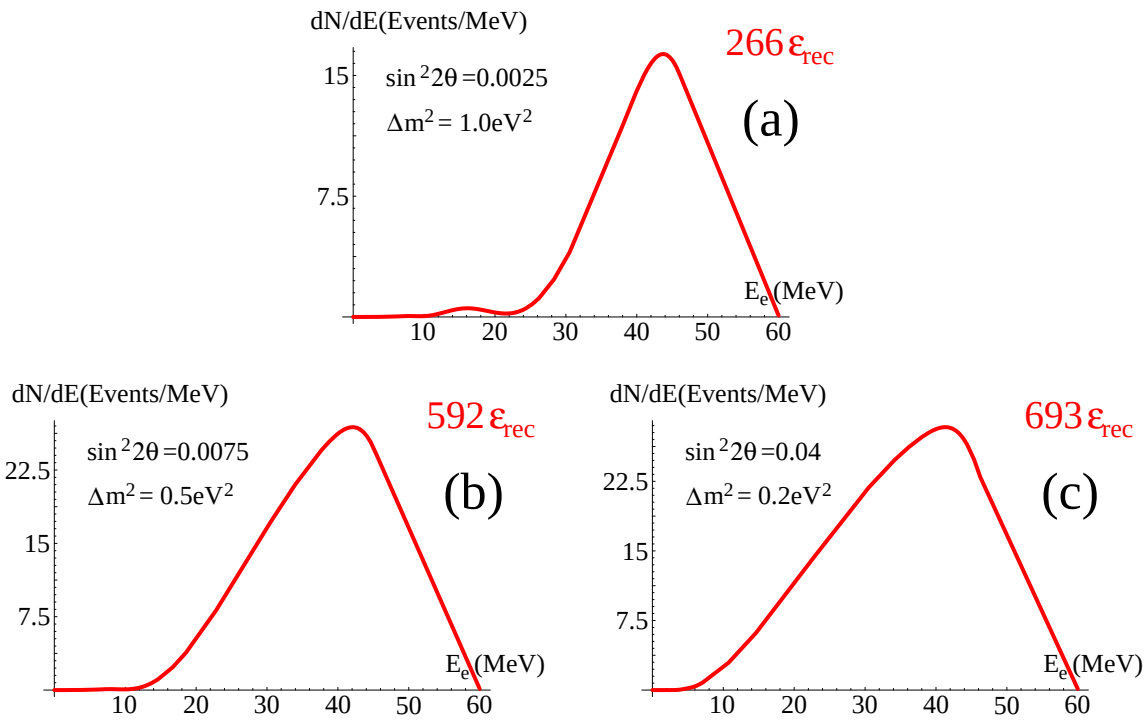

FIG. 7: DAR $\overline{\nu}_\mu \rightarrow \overline{\nu}_e$ Oscillation Event Energies in 250 ton SNS Detector with Energy Smearing (7% at 50MeV)

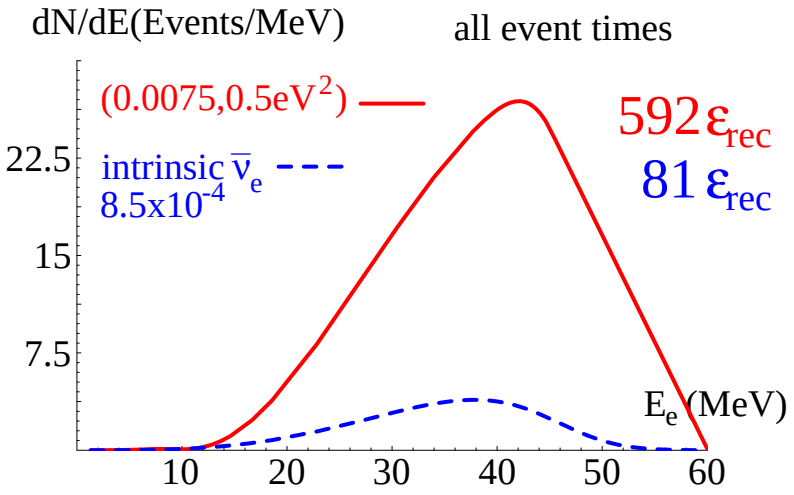

FIG. 8: Intrinsic $\overline{\nu}_e$ Component and $\overline{\nu}_\mu \rightarrow \overline{\nu}_e$ Oscillations with $\sin^2 2\theta = 0.0075$, $\Delta m^2 = 0.5\text{eV}^2$.

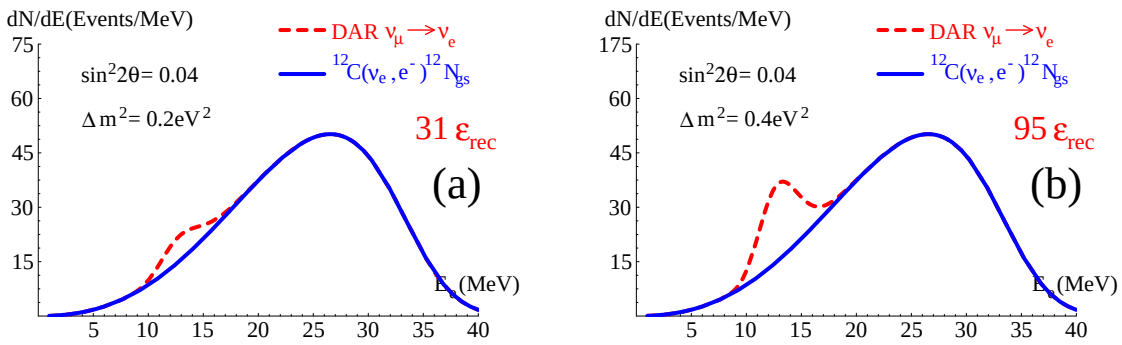

FIG. 9: DAR $\nu_\mu \to \nu_e$ Oscillation Signals for two possible sets of oscillation parameters. (a) For $\sin^2 2\theta = 0.04$, $\Delta m^2 = 0.2\text{eV}^2$, (b) for $\sin^2 2\theta = 0.04$, $\Delta m^2 = 0.4\text{eV}^2$. The background from $^{12}\text{C}(\nu_e, e^-)^{12}\text{N}_{\text{gs}}$ is shown as the solid blue curve. The backgrounds from $^{12}\text{C}(\nu, \nu')^{12}\text{C}^*_{15.11}$ of ~ 15 events peaked at 15.11 MeV is not shown.